We are IntechOpen, the world's leading publisher of Open Access books Built by scientists, for scientists

4,800
Open access books available

122,000
International authors and editors

135M
Downloads

Our authors are among the

154
Countries delivered to

TOP 1%
most cited scientists

12.2%
Contributors from top 500 universities

CLARIVATE ANALYTICS BOOK CITATION INDEX INDEXED

WEB OF SCIENCE™

Selection of our books indexed in the Book Citation Index in Web of Science™ Core Collection (BKCI)

Interested in publishing with us?
Contact book.department@intechopen.com

Numbers displayed above are based on latest data collected.
For more information visit www.intechopen.com

5

Design of Biomimetic Models Related to the Active Sites of Fe-Only Hydrogenase

Yu-Chiao Liu, Ling-Kuang Tu, Tao-Hung Yen and Ming-Hsi Chiang
Institute of Chemistry, Academia Sinica, Taiwan

1. Introduction

Fe-only hydrogenase is a metalloenzyme that is found in a variety of organisms such as acetogenic, photosynthetic, nitrogen-fixing, methanogenic and sulfate reducing bacteria (Adams, 1990; Vignais & Billoud, 2007). It plays an important role on energy cycling in the biological systems. Fe-only hydrogenase can either metabolize hydrogen molecules to produce reducing equivalents or store reducing power in the format of molecular hydrogen (Fontecilla-Camps et al., 2007). The most intriguing part of Fe-only hydrogenase is its high efficiency (6×10^3 s^{-1}) in H_2 production at a mild potential (-0.1 to -0.5 V vs NHC) (Holm et al., 1996). Understanding mechanism of enzymatic hydrogen production will facilitate design of better biomimetic models of Fe-only hydrogenase for substitutes to expensive platinum working electrodes used in industrial hydrogen production (Cammack et al., 2001; Vincent et al., 2007).

$$2\,H^+ \;+\; 2\,e^- \;\leftrightarrow\; H_2 \qquad (1)$$

Recent structural characterization of Fe-only hydrogenase isolated from *Clostridium pasteurianum* (CpI) (Peters et al., 1998) and *Defulfovibrio desulfuricans* (DdH) (Nicolet et al., 1999) shows the active site that is a [6Fe6S] unit called the H-cluster consists of a [2Fe2S] subunit including two square-pyramidal Fe centers bridged by a dithiolate ligand, and a [4Fe4S] cluster (Fig. 1). These [2Fe2S] and [4Fe4S] clusters are linked to each other via a cysteinyl thiolate on the peptide chain. In addition to the S^{cys} bridge, several cyanide and

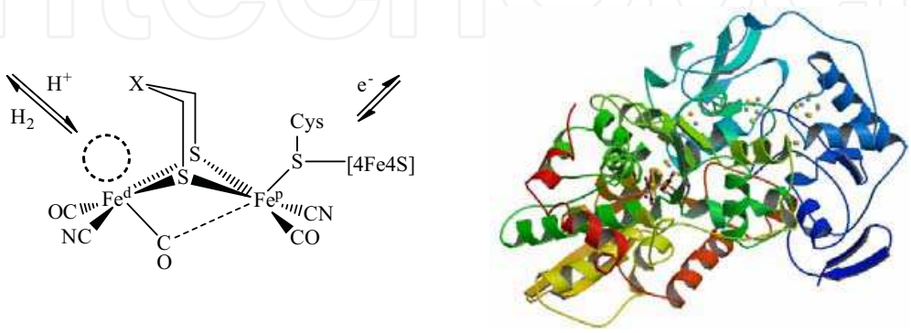

Fig. 1. Protein structure of Fe-only hydrogenase from *Clostridium pasteurianum* (1FEH) (Peters et al., 1998) on the right and the Chemdraw structure of the active site on the left.

carbonyl ligands occupy the primary coordination sphere of the diiron unit. The dithiolate bridge is an abiological ligand that is presumed to dithiomethyl amine ($HN(CH_2S)_2$) (Nicolet et al., 2001; Silakov et al., 2009). Two CN^- groups are arranged in the trans configuration and form hydrogen bonding to nearby amino residues of the peptide backbone. One metal-metal bond is present between two low-spin Fe^l centers that are separated by 2.5-2.6 Å. One vacant site is open to coordination of substrates at the Fe^d center that is the metal site distal to the [4Fe4S] ferredoxin cluster. To the trans position of the catalytic site one CO ligand within the Fe_2 subunit coordinates underneath the Fe-Fe vector for a possible function: distributing electron density between two Fe centers.

When protons are transported through a proton channel within the protein to the active site of Fe-only hydrogenase, the aza nitrogen site being a Lewis base relays protons to the catalytic Fe center as the N-protonated (NH) (Ezzaher et al., 2009; Wang et al., 2005; Wang et al., 2008) and the N-protonated, Fe-hydride (NHFeH) intermediates are generated (Barton et al., 2008; Chiang et al., 2009; Siegbahn et al., 2007) (Fig. 2). Migration of the NH protons is probably initiated by agostic interaction. Another advantage to have the aza nitrogen within the active site of Fe-only hydrogenase is decrease of the reduction potential upon protonation of the N sites (Capon et al., 2008; Liu et al., 2010). In the recent studies of model complexes, the protonated Fe adt (adt = azadithiolate) derivative is reduced at -1.82 V compared with -2.43 V of the un-protonated species (Chiang et al., 2009). Such energy difference as well as ability of proton relays is the reason for protein crystallographers and chemists to choose nitrogen as the putative bridgehead over oxygen and carbon atoms since they are not distinguishable in crystallography (Nicolet et al., 1999; Pandey et al., 2008). In the reversible reaction, the lone pair of the aza nitrogen site assists heterolytic cleavage of molecular hydrogen as the catalytic Fe acts as a Lewis acidic site (Olsen et al., 2009).

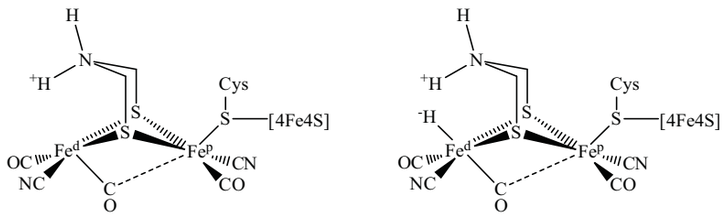

Fig. 2. Possible intermediates in mechanism of enzymatic H_2 production by Fe-only hydrogenase.

If the aza nitrogen site is to assist the enzymatic H_2 production/uptake, availability of the vacant site on the nearby Fe center is a compliment necessity for the high catalytic turnover frequency of the entatic state. Isolation of the model complexes possessing the azadithiolate bridges has been successfully accomplished (Lawrence et al., 2001; Li & Rauchfuss, 2002; Ott et al., 2004). On the contrary, difficulties have been encountered when the model compounds with the apical empty site are prepared *albeit* few unstable examples have been reported.

The organometallic complexes composed of {2Fe2S} moiety have been extensively studied in the recent years (Darensbourg et al., 2003; Tard & Pickett, 2009). Numerous synthetic routes have been developed to better approach the active site of Fe-only hydrogenase (Tard et al., 2005). CO substitution by cyanides, phosphines and other σ-/π-donors are performed in order to enrich electron density about the Fe centers (Lawrence et al., 2001; Liu et al., 2005; Lyon et al., 1999). H_2 production in the presence of these synthetic models is studied by

voltammetric techniques such as cyclic voltammetry and controlled-potential electrolysis (Capon et al., 2009; Capon et al., 2005; Ezzaher et al., 2009; Felton et al., 2009). Unfortunately, the hydride within the identifiable Fe-hydride species is in the bridging fashion for most of the examples (Gloaguen & Rauchfuss, 2009; Greco et al., 2007). The most possible mechanism for formation of the μ-hydride products is addition of protons to the electron enriched Fe-Fe orbitals (Gloaguen et al., 2001). Theoretical calculations have shown that greater activation energy is required to generate the hydride in the terminal manner and the *t*-hydride species is less stable (Zampella et al., 2009). In order to overcome the kinetic hindrance, the apical empty site is a key component.

When the $\{Fe_2S_2\}$ unit of $Fe_2(SS)(CO)_{6-2x}L_{2x}$ and its derivatives (SS = dithiolate linker) is viewed along the Fe-Fe axis, two $Fe(CO)_{3-x}L_x$ moieties are in eclipse configuration. If one of the $Fe(CO)_{3-x}L_x$ moieties is twisted and one of its CO ligands is located underneath the Fe-Fe vector, the apical site on the Fe center is opened up. In this chapter, we would like to deal with the "rotated" structure of the diiron dithiolato carbonyl complexes. Factors that are in control of the rotated geometry will be discussed.

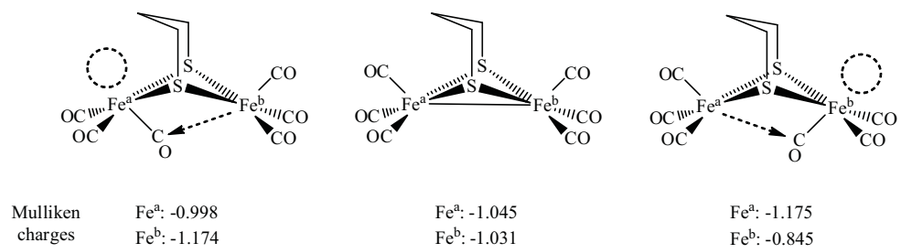

Fig. 3. Changes of Mulliken charges of the Fe centers upon rotation of the Fe^a and Fe^b sites (Georgakaki et al., 2003).

2. The rotated structure

The computed results for the optimized structure of $[Fe_2(\mu\text{-pdt})(CO)_6]$ (pdt = 1,3-propanedithiolate) that agree with the experimentally determined data show electronic equivalence between two metal centers (Georgakaki et al., 2003). The Mulliken charges for both Fe sites are -1.045 and -1.031. HOMO of the ground state structure is predominated by Fe-Fe bond character with symmetric metal contribution, shown in Fig. 3. Once one of the $Fe(CO)_3$ moieties is rotated by 60°, the Fe-Fe bond is disrupted and its distance increases by 0.07 Å. Asymmetric Mulliken charges are obtained as the Fe site of the rotated subunit becomes more positive. In the unrotated structure, all ∠Fe-C-O are nearly 180° whereas ∠Fe-C-O(semi-bridged) is decreased to as small as 168° as the $Fe(CO)_3$ unit is rotated and a semi-bridging CO group is formed. The Fe•••CO(semi) distance is determined to 2.67 Å. Such short distance indicates some interaction is present between the Fe center and this carbonyl group. It is expected the more negative unrotated Fe center distributes some degree of electron density to the more positive rotated Fe center via the CO semi-bridge, which probably provides stabilizing incentive to the rotated structure.

In order to determine degree of the distortion between two Fe subunits, two parameters, ψ and Φ, are employed. Crabtree has introduced the ψ angle to evaluate the coordination mode of CO (Crabtree & Lavin, 1986), displayed in Fig. 4. It is defined to the angle between the Fe-Fe vector and the CO group underneath it. A typical ψ value around 100° is observed

for the terminal carbonyl, whereas it decreases as the carbonyl spins about the Fe-Fe axis to form a CO semi-bridge as the CO continues approaching the second Fe center. A symmetrically coordinated and bent CO bridge (∠Fe-C-O(bri) ≈ 140°) is formed eventually. The second parameter introduced by Darensbourg is the Φ angle which is defined as the torsion angle of L_{ap}-Fe-Fe-L_{ap} (L_{ap} = the apical ligand) (Singleton et al., 2008).

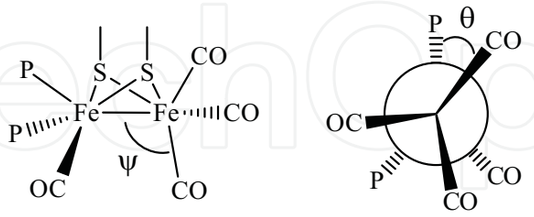

Fig. 4. Schematic presentations of the ψ and Φ angles.

3. Electronic asymmetry

3.1 Electronic asymmetry created by inequivalent substitution

As indicated by DFT calculations (Georgakaki et al., 2003), the structure in the lower energy consists of apical substitution when one CO group is replaced by a σ-donating ligand. Owing to the steric repulsion of the bridgehead the conformer with an apical σ donor at the less hindered side has the lowest energy. This species also has the smallest activation energy for rotation of the $Fe(CO)_3$ subunit among all isomers of $[Fe_2(\mu\text{-pdt})(CO)_5(CN)]$. It suggests the Fe•••CO(semi) interaction is enhanced and the semi-bridging CO is stabilized in the presence of the apical σ donor. Addition of a substrate is then favored if so. In fact, mono-cyanation of $[Fe_2(CO)_5\{MeSCH_2C(Me)(CH_2S)_2\}]$ occurs at a rate 10^4 times faster than the same reaction for $[Fe_2(CO)_6\{CH_2(CH_2S)_2\}]$ (Zampella et al., 2005). The former has a thioether coordinated to the trans position of the Fe-Fe bond in contrast to the all-CO environment of the latter. This apical coordination facilitates facile turnstile rotation of the adjacent $Fe(CO)_3$ subunit to accept CN^- coordination. In this associative mechanism, one bridging/semi-bridging CO intermediate is generated, which has been spectroscopically characterized (Razavet et al., 2001). Besides, it would be interesting to compare the reaction rate for the complex with mono-substitution at the basal position. Only small amount of the di-cyanide product is formed when $[Fe_2(CO)_5(CN)\{MeSCH_2C(Me)(CH_2S)_2\}]$ reacts with cyanide (George et al., 2002). In this molecule, the thioether group is merely a dangling end. Less electron density supplied by the basal cyanide to LUMO of the Fe_2 core makes rupture of the Fe-Fe bond more difficult so the $Fe(CO)_3$ rotation is hindered. In addition, formation of the semi-bridging CO is destabilized. It is found that 300-fold excess of cyanide is required to force clean formation of the di-cyanide species. These results emphasize importance of the apical substitution within $[Fe_2(\mu\text{-SS})(CO)_5L]$.

As appropriate bidentate ligands are employed, larger asymmetric electronic environment is created since the $Fe(CO)L_2$ moiety is much electron-enriched. Greater tendency to constitute the inverted geometry is observed for a few known examples. Compared to $[Fe_2(\mu\text{-pdt})(CO)_6]$, PMe_3 substitution occurs at the faster rate for $[Fe_2(\mu\text{-pdt})(CO)_4(\kappa^2\text{-dppv})]$ (dppv = *cis*-1,2-bis(diphenylphosphino)ethylene) (Justice et al., 2007). It is estimated the rotated transition state is stabilized by 5 kcal/mol in the presence of dppv. On the contrary, the complexes with symmetrically di-substitution are generally inert toward further substitution.

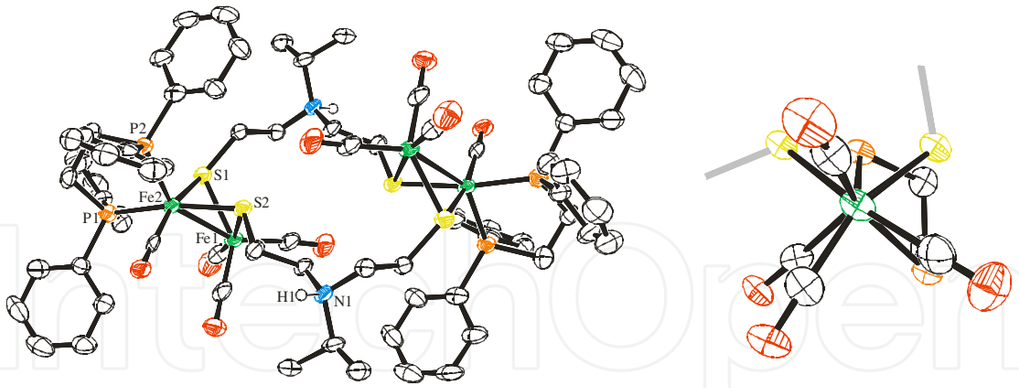

Fig. 5. Molecular structures of $[Fe_2(\mu\text{-}S(CH_2)_2N^iPr(H)(CH_2)_2S)(CO)_4(\kappa^2\text{-}dppe)]_2^{2+}$, thermal ellipsoids drawn at 30% probability level. All hydrogen atoms are omitted for clarity. The side view of partial molecular structure is shown to highlight the distortion.

Computational analysis has shown the highest-energy and lowest-energy IR bands of carbonyls are associated with the $Fe(CO)_3$ and $Fe(CO)L_2$ moieties, respectively, in $[Fe_2(\mu\text{-}SS)(CO)_4(\kappa^2\text{-}P_2)]$ (P_2 = diphosphine chelates) (Justice et al., 2007). The energy difference, $\Delta\nu_{CO}$, therefore can be treated as an approximate gauge of electronic asymmetry between two Fe subunits and act a compliment to the ψ and Φ angles. For the complexes with inequivalent phosphine substitution, the $\Delta\nu_{CO}$ value is commonly greater than 100 cm^{-1} (Justice et al., 2007; Liu et al., 2010; Song et al., 2005; Wang et al., 2008). On the other hand, smaller energy difference of 70-90 cm^{-1} is observed for the symmetrical diphosphine species (Gao et al., 2007; Li et al., 2007). Among the known phosphine-substituted complexes, $[Fe_2(\mu\text{-}S(CH_2)_2N^iPr(Me)(CH_2)_2S)(CO)_4(\kappa^2\text{-}dppe)]_2^{2+}$ (dppe = 1,2-bis(diphenylphosphino)ethane) is the only κ²-diphosphine example with the most distorted structure, characterized by crystallography, where the ψ and Φ angles are 85.9° and 36.3°, respectively. Other than its related derivative, $[Fe_2(\mu\text{-}S(CH_2)_2N^iPr(H)(CH_2)_2S)(CO)_4(\kappa^2\text{-}dppe)]_2^{2+}$ with ψ = 91.4°, no example has an angle smaller or close to 90°. The Φ angle of the same molecule is measured to 34.1° (Fig. 5). The $\Delta\nu_{CO}$ value for both complexes is about 120 cm^{-1}. These results rank these two complexes to the top two examples for the most twisted $Fe(CO)_{3-x}P_x$ configuration. Two other complexes are also reported to possess the large Φ angle: 30.2° and 27.7° for $[Fe_2(\mu\text{-}edt)(CO)_4(\kappa^2\text{-}dppv)]$ (edt = 1,2-ethanedithiolate) (Justice et al., 2007) and $[Fe_2(\mu\text{-}pdt)(CO)_4(\kappa^2\text{-}dppm)]$ (dppm = bis(diphenylphosphino)methane) (Adam et al., 2007), respectively. The two phosphine ends in these complexes occupy the apical and basal positions within one Fe center, which would probably assist rotation of the different Fe subunit.

Free energy profile reveals how the electronic factor dictates the reaction mechanism and products upon protonation of $[Fe_2(\mu\text{-}SS)(CO)_{6-x}P_x]$ (Zampella et al., 2009), as shown in Table 1. For both of the all-CO and di-substituted species, a high activation is required to form a μ-hydride product. This species in addition is thermodynamically disfavored for the former but is stable for the latter. Even so, no computed energy-minimum *t*-hydride structure can be reached for both cases. In other words, the more electron enriched metal centers are required to achieve the goal. In solution, no protonation proceeds unless the all-CO species is reduced first. Formation of the *t*-hydride intermediates are characterized by spectroscopy in the reaction of $[Fe_2(\mu\text{-}pdt)(CO)_4(\kappa^2\text{-}dppe)]$ with HBF_4 (Ezzaher et al., 2007). Two species with hydrides located at either the all-CO or the P-substituted Fe portion are observed at the temperature below 220 K. They quickly convert to the μ-isomer as the temperature is

increased to above 243 K. The experimental results are well consistent with the computed data. Additional phosphine substitution can significantly reduce the reaction energy barrier of protonation. In the presence of four phosphine ligands, $\Delta G^{\ddagger}$ is lowered by about 10 kcal/mol. The *t*-hydride products become stable thermodynamically. The most striking point is formation of the *t*- and μ-hydrides is now kinetically equally favored. $[Fe_2(\mu\text{-pdt})(CO)_2(\kappa^2\text{-dppv})_2]$ reacts with HBF_4 to generate the *t*-hydride product, which is slowly converted to its most stable species of the μ-form (Barton & Rauchfuss, 2008). Similarly, a small rate constant of 2×10^{-4} s^{-1} (294 K) is measured for the intramolecular isomerization of $[Fe_2(\mu\text{-edt})(CO)(\mu\text{-CO})(H)(PMe_3)_4]^+$ to the μ-species (van der Vlugt et al., 2005). Inequivalent (3+1) substitution favors the terminal protonation route *albeit* the bridging form remains the thermodynamically more stable product.

	μ-hydride		*t*-hydride	
	ΔG	$\Delta G^{\ddagger}$	ΔG	$\Delta G^{\ddagger}$
$[(CO)_3Fe(\mu\text{-edt})Fe(CO)_3]$	11.3	17.1	-	-
$[(CO)_3Fe(\mu\text{-edt})Fe(CO)(PH_3)_2]$	-2.3	18.9	-	-
$[(PH_3)_2(CO)Fe(\mu\text{-edt})Fe(CO)(PH_3)_2]$	-13.3	8.1	-3.4	10.9
$[(PH_3)(CO)_2Fe(\mu\text{-edt})Fe(PH_3)_3]$	-19.4	6.0	-8.1	0.0

Table 1. Kinetic and thermodynamic data for formation of the μ- and *t*-hydride species, as energies in kcal/mol (Zampella et al., 2009).

A different class of the complexes with asymmetric electronic structure consists of nitrosyl substitution. When PMe_3 replaces one CO group of the $Fe(CO)_3$ moiety within $[Fe_2(\mu\text{-pdt})(CO)_4(\kappa^2\text{-dppv})]$, the torsion angle of 30.2° decreases to 9.0° owing to counterbalance of electronic asymmetry by PMe_3 addition (Justice et al., 2007). In the presence of NO^+, a significant twist of 36.1° is observed in $[Fe_2(\mu\text{-pdt})(CO)_3(NO)(\kappa^2\text{-dppv})]^+$ instead (Olsen et al., 2008). The most distorted configuration is observed in a series of diiron dithiolato trimethylphosphine complexes. For $[Fe_2(\mu\text{-xdt})(CO)_3(NO)(PMe_3)_2]^+$ (xdt = edt, pdt) where two PMe_3 ligands occupy the apical and basal positions of two different Fe centers, the ψ angles of 76~81° are obtained (Olsen et al., 2008). When the bis-trans-basal PMe_3 conformer is crystallographically characterized, the smallest ψ angle of 62° is measured (Fig. 6). This is the Fe^IFe^I structure most resemble to the inverted geometry of the active site of Fe-only hydrogenase.

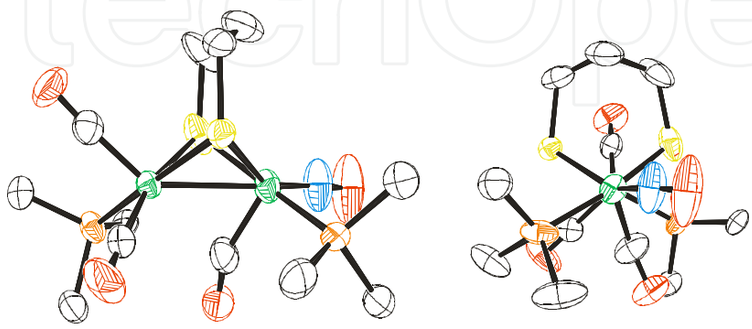

Fig. 6. Molecular structures of $[Fe_2(\mu\text{-pdt})(CO)_3(NO)(PMe_3)_2]^+$, thermal ellipsoids drawn at 35% probability level (Olsen et al., 2008). The side view of molecular structure is shown to highlight the distortion. All hydrogen atoms are omitted for clarity.

3.2 The mixed-valence structures

In addition to tuning by ligand management, the most straightforward route to create an electronic asymmetry is formation of the mixed-valence structures. Single-electron reduction of the $Fe^{I}Fe^{I}$ complexes causes CO liberation (Darchen et al., 1988) in accompany to Fe-S bond cleavage (Borg et al., 2008). The products such as $[Fe_2(\mu,\kappa^2\text{-xdt})(\mu\text{-CO})(CO)_5]^-$ (xdt = pdt, edt, bdt; bdt = 1,2-benzenedithiolate) identified by theoretical calculations (Capon et al., 2007; Felton et al., 2009; Felton et al., 2007), $[Fe_2(\mu\text{-pdt})(CO)_6]^-$ spectroscopically characterized (Borg et al., 2004; Borg et al., 2007), and $[(\mu,\kappa^1\text{-pdt})\{Fe_2(\mu\text{-CO})(CO)_6\}\{Fe_2(\mu\text{-pdt})(CO)_5\}]^{2-}$ and $[(\mu\text{-CO})_2\{Fe_2(\mu\text{-pdt})(CO)_4\}_2]^{2-}$ isolated from experiments (Aguirre de Carcer et al., 2006; Best et al., 2007; Borg et al., 2004) have been obtained or proposed (Fig. 7).

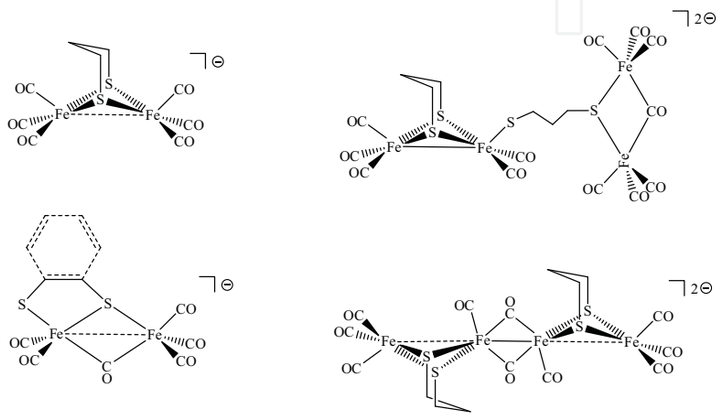

Fig. 7. Single-electron reduction products of the $Fe^{I}Fe^{I}$ species. See the contents for references.

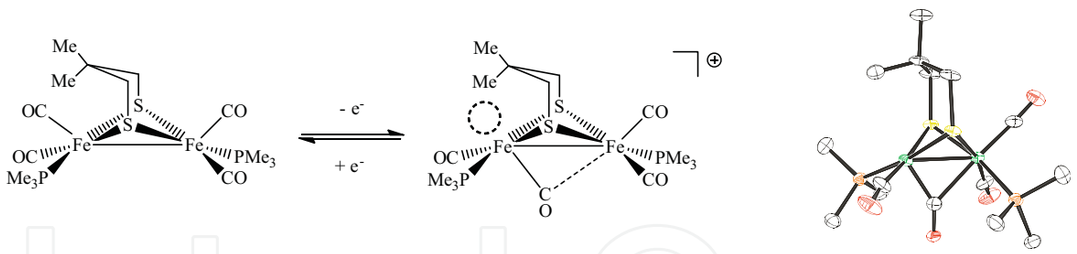

Fig. 8. Synthetic scheme of $[Fe_2(\mu\text{-dmpdt})(\mu\text{-CO})(CO)_3(PMe_3)_2]^+$ and its molecular structure. All hydrogen atoms are omitted for clarity (Singleton et al., 2008).

Successful preparation of the $Fe^{II}Fe^{I}$ complexes has been accomplished at -78 °C (Thomas et al., 2008). These species are only stable at very low temperature. It is assumed the steric influence from either the bulky bridgehead in $[Fe_2(\mu\text{-dmpdt})(CO)_4(PMe_3)_2]$ (dmpdt = 2,2-dimethyl-1,3-propanedithiolate) (Singleton et al., 2008) or the large structural hindrance ligand in $[Fe_2(\mu\text{-pdt})(CO)_4(PMe_3)(IMes)]$ (IMes = 1,3-bis(2,4,6-trimethylphenyl)imidazol-2-ylidene) (Liu & Darensbourg, 2007; Thomas et al., 2008) in addition to the mixed valence assists isolation of the empty apical site (Fig. 8). The ease of oxidation is decreased when additional phosphine ligands replace CO groups of $[Fe_2(\mu\text{-xdt})(CO)_4(\kappa^2\text{-dppv})]$ (Justice et al., 2008). The oxidation potential for $[Fe_2(\mu\text{-edt})(CO)_2(\kappa^2\text{-dppv})_2]$ is -195 mV milder than that of $[Fe_2(\mu\text{-edt})(CO)_3(PMe_3)(\kappa^2\text{-dppv})]$ (Justice et al., 2008). The semi-bridging CO group is characterized in these complexes. The empty apical site is also confirmed by addition of

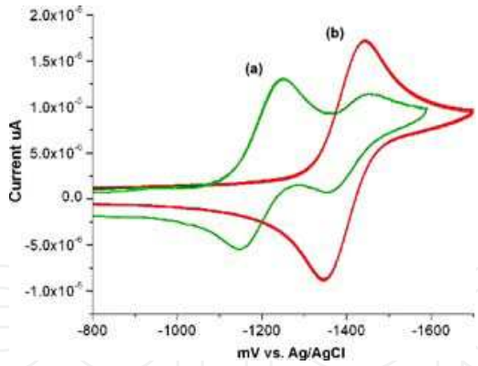

Fig. 9. Cyclic voltammograms of $[Fe_2(\mu\text{-pdt})(H)(CO)_2(\kappa^2\text{-dppv})_2]^+$. (a) a mixture of the *t*- and μ-isomers and (b) the μ-isomer after isomerization (Barton & Rauchfuss, 2008). (copyright 2008 American Chemical Society)

exogenous CO and NO molecules to the first coordination sphere within the $Fe^{II}Fe^{I}$ complex (Justice et al., 2007). The CO adduct product resembles the H_{ox}^{CO} state of the Fe-only hydrogenase. When $[Fe_2\{MeSCH_2C(Me)(CH_2S)_2\}(CN)_2(CO)_4]^{2-}$ is oxidized by one electron, one CO group turns to the bridging mode, which allows the thioether pendant end to coordinate to the apical position (Razavet et al., 2002). The reduction potential can benefit from the presence of the empty apical site as the $Fe^{I}Fe^{I}/Fe^{II}Fe^{I}$ redox event occurs at -0.62 V for $[Fe_2(\mu\text{-pdt})(CO)_4(PMe_3)(IMes)]$ vs -0.10 V for $[Fe_2(\mu\text{-pdt})(CO)_4(PMe_3)_2]$ (Singleton et al., 2008). For the sake of comparison, the *t*-hydride species of $[Fe_2(\mu\text{-pdt})(\mu\text{-CO})(H)(CO)(\kappa^2\text{-dppv})_2]^+$ is reduced at a potential 200 mV milder than its μ-isomer of $[Fe_2(\mu\text{-pdt})(\mu\text{-H})(CO)_2(\kappa^2\text{-dppv})_2]^+$ (Barton & Rauchfuss, 2008), shown in Fig. 9.

4. Bridgehead effects of dithiolate linkers

4.1 Steric influences of the bridgeheads

Significance of the bridgehead's sterics on the activation energy to rotate one $Fe(CO)_3$ moiety in $[Fe_2(\mu\text{-SS})(CO)_6]$ is shown by DFT calculations, where $\Delta G^{\ddagger}$ of 14.10 kcal/mol for $[Fe_2(\mu\text{-edt})(CO)_6]$ is decreased to 13.71 and 12.25 kcal/mol for $[Fe_2(\mu\text{-pdt})(CO)_6]$ and $[Fe_2(\mu\text{-}o\text{-xyldt})(CO)_6]$ (*o*-xyldt = *o*-$C_6H_4(CH_2S)_2$), respectively (Georgakaki et al., 2003). These theoretical results indicate the more hindered bridgehead lowers the barrier to rotation. In the experimental aspects, this factor has been concurred with crystallographical results of a series of $[Fe_2(\mu\text{-SS})(CO)_{6-x}L_x]$ complexes. The Φ angle practically increases from zero in $[Fe_2(\mu\text{-pdt})(CO)_6]$ to 5.7° in $[Fe_2(\mu\text{-dmpdt})(CO)_6]$ (Singleton et al., 2008). A larger Φ value of 15.8° is observed in the bulkier bridgehead derivative, $[Fe_2(\mu\text{-depdt})(CO)_6]$ (depdt = 2,2-diethyl-1,3-propanedithiolate). In addition, a dramatic twist occurs from 4.26° to 40.7° when the pdt bridge in $[Fe_2(\mu\text{-pdt})(CO)_5(IMes)]$ is replaced by the dmpdt bridge. The axial configuration of the butyl substituent in $[Fe_2(\mu\text{-adt})(CO)_4(\mu\text{-dppm})]$ (adt = $BuN(CH_2S)_2$) causes a large torsion angle of 31° compared with 5.2° of $[Fe_2(\mu\text{-pdt})(CO)_4(\mu\text{-dppm})]$ (Gao et al., 2007). Increased steric bulk of the bridgehead leads to larger repulsion between the substituents and the apical carbonyl in the unrotated structure. To lower it, the $Fe(CO)_3$ subunit is forced to spin and eventually a rotated structure in relatively lower energy is obtained (Fig. 10). The calculated ground state energy of the unrotated and rotated optimized structures can be compared. For the smallest substituent, the rotated structure of $[Fe_2(\mu\text{-pdt})(CO)_6]$ is of 12.2 kcal/mol higher than its unrotated parent molecule. This energy

decreases to 9.4 kcal/mol when one proton is replaced by a methyl group (Tye et al., 2006). Large stabilization energy of 4.8 kcal/mol is gained with for a *t*-Bu substituent.

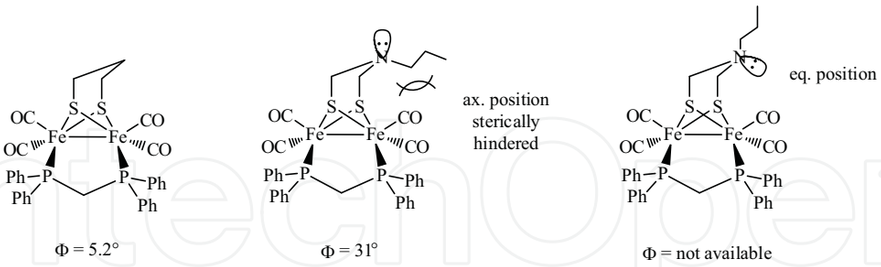

Fig. 10. The Chemdraw structures of $[Fe_2(\mu\text{-xdt})(CO)_4(\mu\text{-dppm})]$ and their corresponding Φ angles (Gao et al., 2007).

Stabilization of the higher energy conformer by the steric hindrance is also observable in the oxidized complexes. In contrast to unavailability of $[Fe_2(\mu\text{-pdt})(CO)_4(PMe_3)_2]^+$, the rotated geometry of $[Fe_2(\mu\text{-dmpdt})(CO)_4(PMe_3)_2]^+$ is stable for structural characterization (Singleton et al., 2008). However, the edt derivative of $[Fe_2(\mu\text{-xdt})(\mu\text{-CO})(CO)_2(PMe_3)(MeCN)(\kappa^2\text{-dppv})]^{2+}$ is robust at room temperature whereas its pdt analogue is merely detectable at low temperature (Justice et al., 2007).

Length of the dithiolate linker has the similar influence to that exerted by the sterically demanding bridgehead. The calculated ground state energy of the rotated structure of $[Fe_2(\mu\text{-S}(CH_2)_nS)(CO)_6]$ is stabilized as *n* is increased (Tye et al., 2006). The rotated conformer is destabilized by 14.7 kcal/mol for $n = 2$. The energy is decreased to 12.2 and 11.6 for $n = 3$ and 4, respectively. For the case of 1,5-pentanedithiolate, the energy is down to 7.4 kcal/mol.

4.2 Lewis acidity and basicity of the bridgehead

When a heteroatom replaces carbon as the central atom of the bridgehead, not only the steric hindrance but also Lewis acidity/basicity affects kinetics and stability of the rotated structure. For the three-atom dithiolate linkers, no variation in energy is observable if the CH_2 group is replaced by the NH group (Tye et al., 2006). The relative short linker length limits any large destabilization caused by the central bridgehead. For the oxa analogue, lacking of the hydrogen atom is probably the reason for its increased ground state energy of the rotamer.

Longer backbones facilitate interaction between the bridgehead and the apical carbonyl of the unrotated structure as well as the metal site of the rotated structure. Among the CH_2, NH and O derivatives of $[Fe_2(\mu\text{-X}(CH_2CH_2S)_2)(CO)_6]$, similar energies are obtained. In contrast, the BH analogue is destabilized by 7.5 kcal/mol. A higher energy of 10.9 kcal/mol is required for its rotated species compared to the lowest-energy NH analogue. It is to say that the electron deficient $\{Fe_2(CO)_6\}$ unit does not accommodate too well with the Lewis acid, i.e. the BH part. On the other hand, to the Lewis acidic units, CO and Fe, the aza nitrogen site forms a good Lewis acid-base pair. Both of its unrotated and rotated structures are of the same energy. A dangling aza nitrogen unit attached to the bridgehead will exert the similar effects on the ground state energy.

In the molecular structures of $[Fe_2(\mu\text{-S}(CH_2)_2NR(CH_2)_2S)(CO)_6]_2$ (R = ^{n}Pr, ^{i}Pr), pointing lone pairs of the aza nitrogens toward the apical carbonyl groups reveals the Fe_2 units are

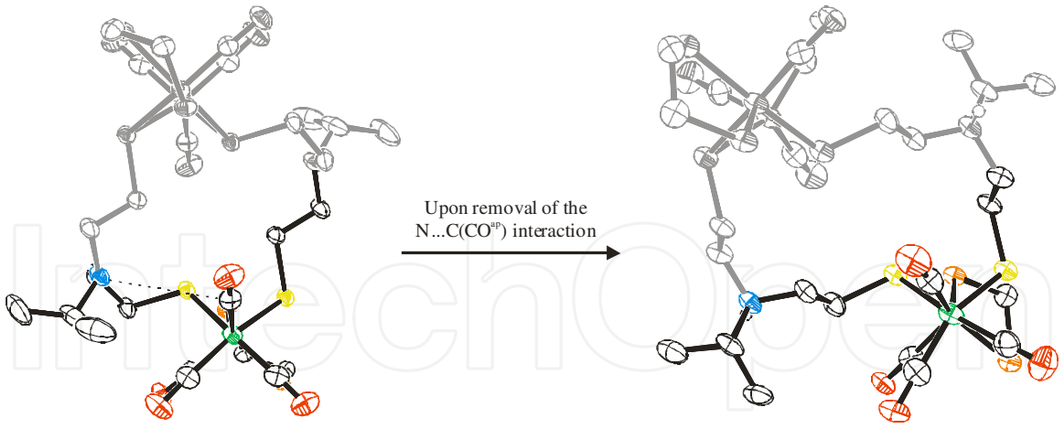

Fig. 11. Presentation of the distortion along the Fe-Fe axis upon removal of the N•••CO(CO^{ap}) interaction within $[Fe_2(\mu\text{-}S(CH_2)_2N^iPr(CH_2)_2S)(CO)_4(\kappa^2\text{-dppe})]_2$. Only the partial molecules are highlighted for the clearer view.

relatively electron poor (Liu et al., 2010). The presence of the N•••CO(CO^{ap}) interaction would assist stabilization of the molecules and function as an indicator of electron richness about the Fe center. The N•••CO(CO^{ap}) distance is increased when CO is substituted by phosphines. The stronger the σ-donating ability, the longer the distance. Besides, this N•••CO(CO^{ap}) interaction could counterbalance electronic asymmetry within the molecule of $[Fe_2(\mu\text{-}S(CH_2)_2N^iPr(CH_2)_2S)(CO)_4(\kappa^2\text{-dppe})]_2$. The distance of 3.721(7) Å is shorter than 4.011(3) Å of the all-CO parent molecule, suggesting a stronger interaction is present. It is probably originated from asymmetric electronic distribution due to the presence of κ^2-dppe so the $Fe(CO)_3$ subunit is more electron deficient than the same part in the all-CO molecule. Unequal distributed electron density is revealed by the distortion angle between two Fe subunits that changes from 10.8° to ~35° upon removal of the N•••CO(CO^{ap}) interaction (Fig. 11). These results stress importance of the aza nitrogen site on the structures.

5. Coordination effect of ligands

5.1 Ligand field caused by the coordinated groups

The active site of Fe-only hydrogenase is encapsulated inside the protein pocket wherein numerous hydrogen bonds between the bound CN^- ligands and the peptide chain are present. Two amino acid residues, Lys^{358} and Ser^{232}, form hydrogen bonds with the CN^- groups of the H-cluster in CpI (Peters et al., 1998). As for DdH, Lys^{237} and the peptide-chain nitrogen atoms of Ala^{109} and Ile^{204} are in close contacts with the cyanides (Nicolet et al., 1999). In addition to the functional role being to modulate electronic structure of the Fe centers, these weak intramolecular interactions serve the structural purpose to support the H-cluster. The peptide backbone that is in control of the rotated geometry of the active site probably via hydrogen bonding would slightly adjust the twist as morphology of the protein changes to adopt the optimal stereo configuration during catalysis. In the synthetic aspects, the di-phosphine bridges with an appropriate length in $[Fe_2(\mu\text{-}SS)(CO)_4P_2]$ can well resemble a combination of cyanides and the peptide chain as the donor ends and the chain backbone are already present. Their donor ability can be tuned by different substituents on the phosphines (Fig. 12).

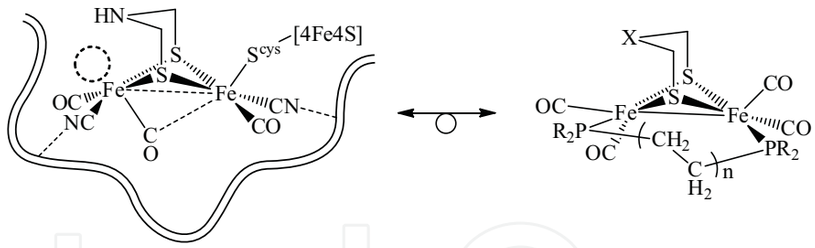

Fig. 12. Schematic presentation of the structural resemblance between the active site and the model complexes.

The distortion angles in $[Fe_2(\mu\text{-}S(CH_2)_2N^iPr(CH_2)_2S)(CO)_4(\mu\text{-}PP)]_2$ (PP = dppe, dppm) can be compared. For the shorter phosphine, the $Fe_2(CO)_4P_2$ unit with a dppm bridge has the more compact structure: 2.522 and 2.549 Å for the Fe-Fe bond distances in $[Fe_2(\mu\text{-}S(CH_2)_2N^iPr(CH_2)_2S)(CO)_4(\mu\text{-dppm})]_2$ and its dppe analogue, respectively (Liu et al., 2010). Since dppm is a relatively rigid bridging ligand, only the eclipse configuration between two Fe moieties is allowed to be achieved. The Φ angle and N•••CO(CO^{ap}) distance of the dppm derivative therefore is comparable to those of the all-CO parent molecule: 3.9 vs 6.0° and 3.987(7) vs 4.011(3) Å for $[Fe_2(\mu\text{-}S(CH_2)_2N^iPr(CH_2)_2S)(CO)_4(\mu\text{-dppm})]_2$ and $[Fe_2(\mu\text{-}S(CH_2)_2N^iPr(CH_2)_2S)(CO)_6]_2$, respectively. The other dppm example, Φ = 5.2° for $[Fe_2(\mu\text{-pdt})(\mu\text{-dppm})(CO)_4]$, is reported (Gao et al., 2007).

Dppe, on the other hand, consists of a two-carbon backbone, giving it higher degree of freedom to adopt the least strained structure in $[Fe_2(\mu\text{-}S(CH_2)_2N^iPr(CH_2)_2S)(CO)_4(\mu\text{-dppe})]_2$. The distances between two phosphorus atoms of 3.787 Å within the Fe_2 subunits is longer than those of the two basal carbonyl carbons and Fe-Fe bond of 3.137 and 2.549 Å, respectively. Combined with assistance of the N•••CO(CO^{ap}) interaction (d = 3.721(7) Å), two Fe moieties are twisted by 26.5°. The most distorted structure from employment of phosphine ligands is observed in $[Fe_2(\mu\text{-pdt})(CO)_3(\mu,\kappa^2\text{-triphos})]$ (triphos = bis(2-diphenylphosphinoethyl)phenylphosphine) (Adam et al., 2007). In this molecule, two phosphorus ends occupy the apical and basal positions of one Fe site while the third phosphorus coordinates to the basal site of the other Fe center in a cis fashion. The Φ and ψ angles of the triphos complex are measured to 49.4 and 88°, respectively. A combined influence from the bridging and chelating manner is expected to result in the large distortion.

5.2 Influences of the secondary coordination sphere interactions

As described in the previous section in which the N•••CO(CO^{ap}) interaction exerts observable impacts on the structure, influences of the second coordination sphere interaction should not be neglected. In the presence of Lewis acids, $AlBr_3$ adduct of $[Fe_2(\mu\text{-xdt})(\mu\text{-CO})(dppv)_2(CO)]$ is formed (Justice et al., 2007). Binding of $AlBr_3$ leads to a 80 cm^{-1} shift on the IR band energy, which is as significant as the change upon protonation of the Fe^IFe^I core. In calculations of the $[Fe_2(\mu\text{-adt})(CO)_5(CH_3SH)]$-$AlCl_3$ pair, the rotated structure with an asymmetrical CO bridge bound to $AlCl_3$ is more stable than the unrotated model possessing an adduct of an apical terminal CO group by 1.2 kcal/mol (Lee & Jo, 2009). Assisted by the bridging CO-$AlCl_3$ group, activation energy to transfer the NH proton to the Fe center is as low as 2.6 kcal/mol in the vacuum. In addition, energies of LUMOs in the NH and NHFeH species are decreased, which in turn makes reductions easier. Effects of interactions in the secondary coordination sphere on reduction potentials have been studied

in several classes of metalloproteins such as iron-sulfur proteins (ferredoxins and high-potential iron proteins) (Low & Hill, 2000) and cupredoxins (Berry et al., 2003). A shift of the working potential greater than 1 V is observed.

6. Conclusion

DFT calculations have indicated that high efficiency of H_2 production is associated with formation of the *t*-hydride species. Since protonation can occur either directly onto the Fe-Fe bond or via the relay route by the aza nitrogen bridgehead, suppression of the μ-hydride form could be achieved in the presence of the rotated structure. From theoretical and experimental studies, several factors in the stereochemical and electronic aspects have been examined. It is apprehended that steric influences of bulky dithiolate linkers, availability and strength of back-donation from the unrotated Fe center to the semi-bridging carbonyl, and structural distortion caused by ligand coordination sphere are critical to the transient inverted-geometry species. A challenge we face now is how to make these factors play in harmony within the biomimetic model complexes.

7. Acknowledgments

The work is supported by National Science Council of Taiwan and Academia Sinica.

8. References

Adam, F. I.; Hogarth, G. & Richards, I. (2007). Models of the iron-only hydrogenase: Reactions of $[Fe_2(CO)_6(\mu\text{-pdt})]$ with small bite-angle diphosphines yielding bridge and chelate diphosphine complexes $[Fe_2(CO)_4(\text{diphosphine})(\mu\text{-pdt})]$. *Journal of Organometallic Chemistry*, 692, 3957-3968.

Adam, F. I.; Hogarth, G.; Richards, I. & Sanchez, B. E. (2007). Models of the iron-only hydrogenase: Structural studies of chelating diphosphine complexes $[Fe_2(CO)_4(\mu\text{-pdt})(\kappa^2P,P'\text{-diphosphine})]$. *Dalton Transactions*, 2495-2498.

Adams, M. W. W. (1990). The structure and mechanism of iron-hydrogenases. *Biochimica et Biophysica Acta*, 1020, 115-145.

Aguirre de Carcer, I.; DiPasquale, A.; Rheingold, A., L. & Heinekey, D. M. (2006). Active-site models for iron hydrogenases: Reduction chemistry of dinuclear iron complexes. *Inorganic Chemistry*, 45, 8000-8002.

Barton, B. E.; Olsen, M. T. & Rauchfuss, T. B. (2008). Aza- and oxadithiolates are probable proton relays in functional models for the [FeFe]-hydrogenases. *Journal of the American Chemical Society*, 130, 16834-16835.

Barton, B. E. & Rauchfuss, T. B. (2008). Terminal hydride in [FeFe]-hydrogenase model has lower potential for H_2 production than the isomeric bridging hydride. *Inorganic Chemistry*, 47, 2261-2263.

Berry, S. M.; Ralle, M.; Low, D. W.; Blackburn, N. J. & Lu, Y. (2003). Probing the role of axial methionine in the blue copper center of azurin with unnatural amino acids. *Journal of the American Chemical Society*, 125, 8760-8768.

Best, S. P.; Borg, S. J.; White, J. M.; Razavet, M. & Pickett, C. J. (2007). On the structure of a proposed mixed-valent analogue of the diiron subsite of [FeFe]-hydrogenase. *Chemical Communications*, 4348-4350.

Borg, S. J.; Behrsing, T.; Best, S. P.; Razavet, M.; Liu, X. & Pickett, C. J. (2004). Electron transfer at a dithiolate-bridged diiron assembly: Electrocatalytic hydrogen evolution. *Journal of the American Chemical Society*, 126, 16988-16999.

Borg, S. J.; Ibrahim, S. K.; Pickett, C. J. & Best, S. P. (2008). Electrocatalysis of hydrogen evolution by synthetic diiron units using weak acids as the proton source: Pathways of doubtful relevance to enzymic catalysis by the diiron subsite of [FeFe] hydrogenase. *Comptes Rendus Chimie*, 11, 852-860.

Borg, S. J.; Tye, J. W.; Hall, M. B. & Best, S. P. (2007). Assignment of molecular structures to the electrochemical reduction products of diiron compounds related to [Fe-Fe] hydrogenase: A combined experimental and density functional theory study. *Inorganic Chemistry*, 46, 384-394.

Cammack, R.; Frey, M. & Robson, R. (2001). *Hydrogen as a fuel: Learning from nature*, Taylor & Francis, 0-415-24242-8, London and New York.

Capon, J.-F.; Ezzaher, S.; Gloaguen, F.; Pétillon, F. Y.; Schollhammer, P. & Talarmin, J. (2008). Electrochemical insights into the mechanisms of proton reduction by $[Fe_2(CO)_6\{\mu\text{-}SCH_2N(R)CH_2S\}]$ complexes related to the $[2Fe]_H$ subsite of [FeFe]hydrogenase. *Chemistry-A European Journal*, 14, 1954-1964.

Capon, J.-F.; Ezzaher, S.; Gloaguen, F.; Pétillon, F. Y.; Schollhammer, P.; Talarmin, J.; Davin, T. J.; McGrady, J. E. & Muir, K. W. (2007). Electrochemical and theoretical investigations of the reduction of $[Fe_2(CO)_5L\{\mu\text{-}SCH_2XCH_2S\}]$ complexes related to [FeFe] hydrogenase. *New Journal of Chemistry*, 31, 2052-2064.

Capon, J.-F.; Gloaguen, F.; Pétillon, F. Y.; Schollhammer, P. & Talarmin, J. (2009). Electron and proton transfers at diiron dithiolate sites relevant to the catalysis of proton reduction by the [FeFe]-hydrogenases. *Coordination Chemistry Reviews*, 253, 1476-1494.

Capon, J.-F.; Gloaguen, F.; Schollhammer, P. & Talarmin, J. (2005). Catalysis of the electrochemical H_2 evolution by di-iron sub-site models. *Coordination Chemistry Reviews*, 249, 1664-1676.

Chiang, M.-H.; Liu, Y.-C.; Yang, S.-T. & Lee, G.-H. (2009). Biomimetic model featuring the NH proton and bridging hydride related to a proposed intermediate in enzymatic H_2 production by Fe-only hydrogenase. *Inorganic Chemistry*, 48, 7604-7612.

Crabtree, R. H. & Lavin, M. (1986). Structural analysis of the semibridging carbonyl. *Inorganic Chemistry*, 25, 805-812.

Darchen, A.; Mousser, H. & Patin, H. (1988). Two-electron transfer catalysis of carbon monoxide exchange with a ligand in hexacarbonyldiiron compounds $[(\mu\text{-}RS)_2Fe_2(CO)_6]$. *Journal of the Chemical Society, Chemical Communications*, 968-970.

Darensbourg, M. Y.; Lyon, E. J.; Zhao, X. & Georgakaki, I. P. (2003). The organometallic active site of [Fe]hydrogenase: Models and entatic states. *Proceedings of the National Academy of Sciences of the United States of America*, 100, 3683-3688.

Ezzaher, S.; Capon, J.-F.; Dumontet, N.; Gloaguen, F.; Pétillon, F. Y.; Schollhammer, P. & Talarmin, J. (2009). Electrochemical study of the role of a H-bridged, unsymmetrically disubstituted diiron complex in proton reduction catalysis. *Journal of Electroanalytical Chemistry*, 626, 161-170.

Ezzaher, S.; Capon, J.-F.; Gloaguen, F.; Pétillon, F. Y.; Schollhammer, P.; Talarmin, J. & Kervarec, N. (2009). Influence of a pendant amine in the second coordination

sphere on proton transfer at a dissymmetrically disubstituted diiron system related to the $[2Fe]_H$ Subsite of $[FeFe]H_2$ase. *Inorganic Chemistry*, 48, 2-4.

Ezzaher, S.; Capon, J.-F.; Gloaguen, F.; Pétillon, F. Y.; Schollhammer, P.; Talarmin, J.; Pichon, R. & Kervarec, N. (2007). Evidence for the formation of terminal hydrides by protonation of an asymmetric iron hydrogenase active site mimic. *Inorganic Chemistry*, 46, 3426-3428.

Felton, G. A. N.; Mebi, C. A.; Petro, B. J.; Vannucci, A. K.; Evans, D. H.; Glass, R. S. & Lichtenberger, D. L. (2009). Review of electrochemical studies of complexes containing the Fe_2S_2 core characteristic of [FeFe]-hydrogenases including catalysis by these complexes of the reduction of acids to form dihydrogen. *Journal of Organometallic Chemistry*, 694, 2681-2699.

Felton, G. A. N.; Petro, B. J.; Glass, R. S.; Lichtenberger, D. L. & Evans, D. H. (2009). One- to two-electron reduction of an [FeFe]-hydrogenase active site mimic: The critical role of fluxionality of the [2Fe2S] core. *Journal of the American Chemical Society*, 131, 11290-11291.

Felton, G. A. N.; Vannucci, A. K.; Chen, J.; Lockett, L. T.; Okumura, N.; Petro, B. J.; Zakai, U. I.; Evans, D. H.; Glass, R. S. & Lichtenberger, D. L. (2007). Hydrogen generation from weak acids: Electrochemical and computational studies of a diiron hydrogenase mimic. *Journal of the American Chemical Society*, 129, 12521-12530.

Fontecilla-Camps, J. C.; Volbeda, A.; Cavazza, C. & Nicolet, Y. (2007). Structure/function relationships of [NiFe]- and [FeFe]-hydrogenases. *Chemical Reviews*, 107, 4273-4303.

Gao, W.; Ekströem, J.; Liu, J.; Chen, C.; Eriksson, L.; Weng, L.; Åkermark, B. & Sun, L. (2007). Binuclear iron-sulfur complexes with bidentate phosphine ligands as active site models of Fe-hydrogenase and their catalytic proton reduction. *Inorganic Chemistry*, 46, 1981-1991.

Georgakaki, I. P.; Thomson, L. M.; Lyon, E. J.; Hall, M. B. & Darensbourg, M. Y. (2003). Fundamental properties of small molecule models of Fe-only hydrogenase: Computations relative to the definition of an entatic state in the active site. *Coordination Chemistry Reviews*, 238-239, 255-266.

George, S. J.; Cui, Z.; Razavet, M. & Pickett, C. J. (2002). The di-iron subsite of all-iron hydrogenase: Mechanism of cyanation of a synthetic {2Fe3S} - carbonyl assembly. *Chemistry-A European Journal*, 8, 4037-4046.

Gloaguen, F.; Lawrence, J. D. & Rauchfuss, T. B. (2001). Biomimetic hydrogen evolution catalyzed by an iron carbonyl thiolate. *Journal of the American Chemical Society*, 123, 9476-9477.

Gloaguen, F. & Rauchfuss, T. B. (2009). Small molecule mimics of hydrogenases: Hydrides and redox. *Chemical Society Reviews*, 38, 100-108.

Greco, C.; Zampella, G.; Bertini, L.; Bruschi, M.; Fantucci, P. & De Gioia, L. (2007). Insights into the mechanism of electrocatalytic hydrogen evolution mediated by $Fe_2(S_2C_3H_6)(CO)_6$: The simplest functional model of the Fe-hydrogenase active site. *Inorganic Chemistry*, 46, 108-116.

Holm, R. H.; Kennepohl, P. & Solomon, E. I. (1996). Structural and functional aspects of metal sites in biology. *Chemical Reviews*, 96, 2239-2314.

Justice, A. K.; De Gioia, L.; Nilges, M. J.; Rauchfuss, T. B.; Wilson, S. R. & Zampella, G. (2008). Redox and structural properties of mixed-valence models for the active site

of the [FeFe]-hydrogenase: Progress and challenges. *Inorganic Chemistry*, 47, 7405-7414.

Justice, A. K.; Nilges, M. J.; Rauchfuss, T. B.; Wilson, S. R.; De Gioia, L. & Zampella, G. (2008). Diiron dithiolato carbonyls related to the H_{ox}^{CO} state of [FeFe]-hydrogenase. *Journal of the American Chemical Society*, 130, 5293-5301.

Justice, A. K.; Rauchfuss, T. B. & Wilson, S. R. (2007). Unsaturated, mixed-valence diiron dithiolate model for the H_{ox} state of the [FeFe] hydrogenase. *Angewandte Chemie International Edition*, 46, 6152-6154.

Justice, A. K.; Zampella, G.; De Gioia, L. & Rauchfuss, T. B. (2007). Lewis vs. Brønsted-basicities of diiron dithiolates: spectroscopic detection of the "rotated structure" and remarkable effects of ethane-vs. propanedithiolate. *Chemical Communications*, 2019-2021.

Justice, A. K.; Zampella, G.; De Gioia, L.; Rauchfuss, T. B.; van der Vlugt, J. I. & Wilson, S. R. (2007). Chelate control of diiron(I) dithiolates relevant to the [Fe-Fe]-hydrogenase active site. *Inorganic Chemistry*, 46, 1655-1664.

Lawrence, J. D.; Li, H. & Rauchfuss, T. B. (2001). Beyond Fe-only hydrogenases: *N*-functionalized 2-aza-1,3-dithiolates $Fe_2[(SCH_2)_2NR](CO)_x$ (x = 5, 6). *Chemical Communications*, 1482-1483.

Lawrence, J. D.; Li, H.; Rauchfuss, T. B.; Bénard, M. & Rohmer, M.-M. (2001). Diiron azadithiolates as models for the iron-only hydrogenase active site: Synthesis, structure, and stereoelectronics. *Angewandte Chemie International Edition*, 40, 1768-1771.

Lee, J. W. & Jo, W. H. (2009). Effect of Lewis acid on the structure of a diiron dithiolate complex based on the active site of [FeFe]-hydrogenase assessed by density functional theory. *Dalton Transactions*, 8532-8537.

Li, H. & Rauchfuss, T. B. (2002). Iron carbonyl sulfides, formaldehyde, and amines condense to give the proposed azadithiolate cofactor of the Fe-only hydrogenases. *Journal of the American Chemical Society*, 124, 726-727.

Li, P.; Wang, M.; He, C.; Liu, X.; Jin, K. & Sun, L. (2007). Phosphane and phosphite unsymmetrically disubstituted diiron complexes related to the Fe-only hydrogenase active site. *European Journal of Inorganic Chemistry*, 3718-3727.

Liu, T. & Darensbourg, M. Y. (2007). A mixed-valent, Fe(II)Fe(I), diiron complex reproduces the unique rotated state of the [FeFe]hydrogenase active site. *Journal of the American Chemical Society*, 129, 7008-7009.

Liu, X.; Ibrahim, S. K.; Tard, C. & Pickett, C. J. (2005). Iron-only hydrogenase: Synthetic, structural and reactivity studies of model compounds. *Coordination Chemistry Reviews*, 249, 1641-1652.

Liu, Y.-C.; Tu, L.-K.; Yen, T.-H.; Lee, G.-H. & Chiang, M.-H. (2010). Submitted.

Liu, Y.-C.; Tu, L.-K.; Yen, T.-H.; Lee, G.-H.; Yang, S.-T. & Chiang, M.-H. (2010). Secondary coordination sphere interactions within the biomimetic iron azadithiolate complexes related to Fe-only hydrogenase: Dynamic measure of electron density about the Fe sites. *Inorganic Chemistry*, 49, 6409-6420.

Low, D. W. & Hill, M. G. (2000). Backbone-Engineered High-Potential Iron Proteins: Effects of Active-Site Hydrogen Bonding on Reduction Potential. *Journal of the American Chemical Society*, 122, 11039-11040.

Lyon, E. J.; Georgakaki, I. P.; Reibenspies, J. H. & Darensbourg, M. Y. (1999). Carbon monoxide and cyanide ligands in a classical organometallic complex model for Fe-only hydrogenase. *Angewandte Chemie International Edition*, 38, 3178-3180.

Nicolet, Y.; De Lacey, A. L.; Vernède, X.; Fernandez, V. M.; Hatchikian, E. C. & Fontecilla-Camps, J. C. (2001). Crystallographic and FTIR spectroscopic evidence of changes in Fe coordination upon reduction of the active site of the Fe-only hydrogenase from Desulfovibrio desulfuricans. *Journal of the American Chemical Society*, 123, 1596-1601.

Nicolet, Y.; Piras, C.; Legrand, P.; Hatchikian, C. E. & Fontecilla-Camps, J. C. (1999). Desulfovibrio desulfuricans iron hydrogenase: The structure shows unusual coordination to an active site Fe binuclear center. *Structure*, 7, 13-23.

Olsen, M. T.; Barton, B. E. & Rauchfuss, T. B. (2009). Hydrogen activation by biomimetic diiron dithiolates. *Inorganic Chemistry*, 48, 7507-7509.

Olsen, M. T.; Bruschi, M.; De Gioia, L.; Rauchfuss, T. B. & Wilson, S. R. (2008). Nitrosyl derivatives of diiron(I) dithiolates mimic the structure and Lewis acidity of the [FeFe]-hydrogenase active site. *Journal of the American Chemical Society*, 130, 12021-12030.

Olsen, M. T.; Justice, A. K.; Gloaguen, F.; Rauchfuss, T. B. & Wilson, S. R. (2008). New nitrosyl derivatives of diiron dithiolates related to the active site of the [FeFe]-hydrogenases. *Inorganic Chemistry*, 47, 11816-11824.

Ott, S.; Kritikos, M.; Åkermark, B.; Sun, L. & Lomoth, R. (2004). A biomimetic pathway for hydrogen evolution from a model of the iron hydrogenase active site. *Angewandte Chemie International Edition*, 43, 1006-1009.

Pandey, A. S.; Harris, T. V.; Giles, L. J.; Peters, J. W. & Szilagyi, R. K. (2008). Dithiomethylether as a ligand in the hydrogenase H-cluster. *Journal of the American Chemical Society*, 130, 4533-4540.

Peters, J. W.; Lanzilotta, W. N.; Lemon, B. J. & Seefeldt, L. C. (1998). X-ray crystal structure of the Fe-only hydrogenase (CpI) from Clostridium pasteurianum to 1.8 angstrom resolution. *Science*, 282, 1853-1858.

Razavet, M.; Borg, S. J.; George, S. J.; Best, S. P.; Fairhurst, S. A. & Pickett, C. J. (2002). Transient FTIR spectroelectrochemical and stopped-flow detection of a mixed valence {Fe(I)-Fe(II)} bridging carbonyl intermediate with structural elements and spectroscopic characteristics of the di-iron sub-site of all-iron hydrogenase. *Chemical Communications*, 700-701.

Razavet, M.; Davies, S. C.; Hughes, D. L. & Pickett, C. J. (2001). {2Fe3S} clusters related to the di-iron sub-site of the H-centre of all-iron hydrogenases. *Chemical Communications*, 847-848.

Siegbahn, P. E. M.; Tye, J. W. & Hall, M. B. (2007). Computational studies of [NiFe] and [FeFe] hydrogenases. *Chemical Reviews*, 107, 4414-4435.

Silakov, A.; Wenk, B.; Reijerse, E. & Lubitz, W. (2009). ^{14}N HYSCORE investigation of the H-cluster of [FeFe] hydrogenase: Evidence for a nitrogen in the dithiol bridge. *Physical Chemistry Chemical Physics*, 11, 6592-6599.

Singleton, M. L.; Bhuvanesh, N.; Reibenspies, J. H. & Darensbourg, M. Y. (2008). Synthetic support of de novo design: Sterically bulky [FeFe]-hydrogenase models. *Angewandte Chemie International Edition*, 47, 9492-9495.

Singleton, M. L.; Jenkins, R. M.; Klemashevich, C. L. & Darensbourg, M. Y. (2008). The effect of bridgehead steric bulk on the ground state and intramolecular exchange processes of (μ-$SCH_2CR_2CH_2S$)[$Fe(CO)_3$][$Fe(CO)_2L$] complexes. *Comptes Rendus Chimie*, 11, 861-874.

Song, L.-C.; Yang, Z.-Y.; Bian, H.-Z.; Liu, Y.; Wang, H.-T.; Liu, X.-F. & Hu, Q.-M. (2005). Diiron oxadithiolate type models for the active site of iron-only hydrogenases and biomimetic hydrogen evolution catalyzed by Fe_2(μ-SCH_2OCH_2S-μ)$(CO)_6$. *Organometallics*, 24, 6126-6135.

Tard, C.; Liu, X.; Ibrahim, S. K.; Bruschi, M.; De Gioia, L.; Davies, S. C.; Yang, X.; Wang, L.-S.; Sawers, G. & Pickett, C. J. (2005). Synthesis of the H-cluster framework of iron-only hydrogenase. *Nature*, 433, 610-613.

Tard, C. & Pickett, C. J. (2009). Structural and functional analogues of the active sites of the [Fe]-, [NiFe]-, and [FeFe]-hydrogenases. *Chemical Reviews*, 109, 2245-2274.

Thomas, C. M.; Liu, T.; Hall, M. B. & Darensbourg, M. Y. (2008). Regioselective $^{12}CO/^{13}CO$ exchange activity of a mixed-valent Fe(II)Fe(I) model of the H_{ox} state of [FeFe]-hydrogenase. *Chemical Communications*, 1563-1565.

Thomas, C. M.; Liu, T.; Hall, M. B. & Darensbourg, M. Y. (2008). Series of mixed valent Fe(II)Fe(I) complexes that model the H_{ox} state of [FeFe]hydrogenase: Redox properties, density-functional theory investigation, and reactivities with extrinsic CO. *Inorganic Chemistry*, 47, 7009-7024.

Tye, J. W.; Darensbourg, M. Y. & Hall, M. B. (2006). De novo design of synthetic di-iron(I) complexes as structural models of the reduced form of iron-iron hydrogenase. *Inorganic Chemistry*, 45, 1552-1559.

van der Vlugt, J. I.; Rauchfuss, T. B.; Whaley, C. M. & Wilson, S. R. (2005). Characterization of a diferrous terminal hydride mechanistically relevant to the Fe-only hydrogenases. *Journal of the American Chemical Society*, 127, 16012-16013.

Vignais, P. M. & Billoud, B. (2007). Occurrence, classification, and biological function of hydrogenases: An overview. *Chemical Reviews*, 107, 4206-4272.

Vincent, K. A.; Parkin, A. & Armstrong, F. A. (2007). Investigating and exploiting the electrocatalytic properties of hydrogenases. *Chemical Reviews*, 107, 4366-4413.

Wang, F.; Wang, M.; Liu, X.; Jin, K.; Dong, W.; Li, G.; Åkermark, B. & Sun, L. (2005). Spectroscopic and crystallographic evidence for the N-protonated Fe^IFe^I azadithiolate complex related to the active site of Fe-only hydrogenases. *Chemical Communications*, 3221-3223.

Wang, N.; Wang, M.; Liu, T.; Li, P.; Zhang, T.; Darensbourg, M. Y. & Sun, L. (2008). CO-migration in the ligand substitution process of the chelating diphosphite diiron complex (μ-pdt)[$Fe(CO)_3$][$Fe(CO)\{(EtO)_2PN(Me)P(OEt)_2\}$]. *Inorganic Chemistry*, 47, 6948-6955.

Wang, N.; Wang, M.; Zhang, T.; Li, P.; Liu, J. & Sun, L. (2008). A proton-hydride diiron complex with a base-containing diphosphine ligand relevant to the [FeFe]-hydrogenase active site. *Chemical Communications*, 5800-5802.

Zampella, G.; Bruschi, M.; Fantucci, P.; Razavet, M.; Pickett, C. J. & De Gioia, L. (2005). Dissecting the intimate mechanism of cyanation of {2Fe3S} complexes related to the active site of all-iron hydrogenases by DFT analysis of energetics, transition states, intermediates and products in the carbonyl substitution pathway. *Chemistry-A European Journal*, 11, 509-520.

Zampella, G.; Fantucci, P. & De Gioia, L. (2009). Unveiling how stereoelectronic factors affect kinetics and thermodynamics of protonation regiochemistry in [FeFe] hydrogenase synthetic models: A DFT investigation. *Journal of the American Chemical Society*, 131, 10909-10917.

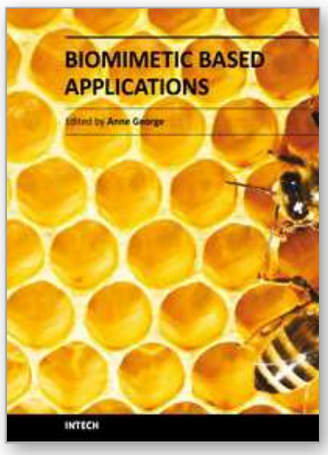

Biomimetic Based Applications

Edited by Prof. Marko Cavrak

ISBN 978-953-307-195-4
Hard cover, 572 pages
Publisher InTech
Published online 26, April, 2011
Published in print edition April, 2011

The interaction between cells, tissues and biomaterial surfaces are the highlights of the book "Biomimetic Based Applications". In this regard the effect of nanostructures and nanotopographies and their effect on the development of a new generation of biomaterials including advanced multifunctional scaffolds for tissue engineering are discussed. The 2 volumes contain articles that cover a wide spectrum of subject matter such as different aspects of the development of scaffolds and coatings with enhanced performance and bioactivity, including investigations of material surface-cell interactions.

How to reference

In order to correctly reference this scholarly work, feel free to copy and paste the following:

Yu-Chiao Liu, Ling-Kuang Tu, Tao-Hung Yen and Ming-Hsi Chiang (2011). Design of Biomimetic Models Related to the Active Sites of Fe-Only Hydrogenase, Biomimetic Based Applications, Prof. Marko Cavrak (Ed.), ISBN: 978-953-307-195-4, InTech, Available from: http://www.intechopen.com/books/biomimetic-based-applications/design-of-biomimetic-models-related-to-the-active-sites-of-fe-only-hydrogenase

INTECH
open science | open minds

InTech Europe
University Campus STeP Ri
Slavka Krautzeka 83/A
51000 Rijeka, Croatia
Phone: +385 (51) 770 447
Fax: +385 (51) 686 166
www.intechopen.com

InTech China
Unit 405, Office Block, Hotel Equatorial Shanghai
No.65, Yan An Road (West), Shanghai, 200040, China
中国上海市延安西路65号上海国际贵都大饭店办公楼405单元
Phone: +86-21-62489820
Fax: +86-21-62489821

IntechOpen